

Human immunodeficiency virus-1 reverse transcriptase heterodimer stability*

JACOB LEBOWITZ,¹ SAMBIT KAR,² EMORY BRASWELL,³ SYLVIA McPHERSON,¹
AND DEAN L. RICHARD¹

¹ Department of Microbiology and Center for AIDS Research, University of Alabama at Birmingham, Birmingham, Alabama 35294

² Biophysical Sciences Graduate Program, University of Alabama at Birmingham, Birmingham, Alabama 35294

³ National Analytical Ultracentrifuge Facility, University of Connecticut, Storrs, Connecticut 06269

(RECEIVED February 2, 1994; ACCEPTED July 25, 1994)

Abstract

Structural and biochemical evidence strongly supports a heterodimeric (p66p51) active form for human immunodeficiency virus-1 reverse transcriptase (RT). Heterodimer stability was examined by sedimentation analysis as a function of temperature and ionic strength. Using NONLIN regression software, monomer-dimer-trimer and monomer-dimer-tetramer association models gave the best fit to the analytical ultracentrifuge sedimentation equilibrium data. The heterodimer is the predominant form of RT at 5 °C, with a dimerization K_a value of $5.2 \times 10^5 \text{ M}^{-1}$ for both models. K_a values of 2.1×10^5 and $3.8 \times 10^5 \text{ M}^{-1}$ were obtained for the respective association models at 20 °C. RT in 50 and 100 mM Tris, pH 7.0, completely dissociates at 37 °C and behaves as an ideal monomeric species. The dissociation of RT as a function of increasing temperature was also observed by measuring the decrease in sedimentation velocity ($s_{w,20}$). If the stabilization of the heterodimer was due primarily to hydrophobic interactions we would anticipate an increase in the association from 21 °C to 37 °C. The opposite temperature dependence for the association of RT suggests that electrostatic and hydrogen bond interactions play an important role in stabilizing heterodimers. To examine the effect of ionic strength on p66p51 association we determined the changes in $s_{w,20}$ as a function of NaCl concentration. There is a sharp decrease in $s_{w,20}$ between 0.10 and 0.5 M NaCl, leading to apparent complete dissociation. The above results support a major role for electrostatic interactions in the stabilization of the RT heterodimer.

Keywords: association constants; electrostatic interactions; heterodimer stability; immunodeficiency virus-1; reverse transcriptase; sedimentation equilibrium; sedimentation velocity

The human immunodeficiency virus (HIV) reverse transcriptase (RT) is the enzyme responsible for the conversion of the viral genome from a single-stranded RNA to double-stranded DNA, which is then integrated into the cellular genome by a viral-coded integrase. RT has been a major target for the treatment of acquired immunodeficiency syndrome (AIDS). The native enzyme has DNA polymerase and RNase H activities and exists as a heterodimer containing polypeptides of approximately 66 and 51 kDa (DiMarzo-Veronese et al., 1986; Lightfoote et al., 1986). The p66 subunit contains both the DNA polymerase and RNase H functional domains, whereas the smaller polypeptide, p51, lacks the carboxyl-terminal RNase H domain (Hansen et al., 1988). RT and the viral DNA integration protein are synthesized as part of the *gag-pol* precursor polyprotein (for review see,

Whitcomb & Hughes, 1992). Cleavage of *gag-pol* polyprotein by the virally encoded protease releases p66, which is capable of forming a weakly associated homodimer (Becerra et al., 1991). Either the homodimer or the p66 monomer is the substrate for additional viral protease processing, which leads to stable p66p51 heterodimers.

Two recent X-ray crystallographic studies of HIV-1 RT have resulted in the 3-dimensional structure of the enzyme, providing a description of the folding and topology of the individual subdomains (Kohlstaedt et al., 1992; Jacobo-Molina et al., 1993; Nanni et al., 1993). The crystal structure analysis of RT at 3.0 Å resolution has delineated 4 subdomains, 3 of which have been designated as fingers, palm, and thumb because the polymerase domain resembles a hand. A connection subdomain joins the polymerase domain to the RNase H domain in the p66 protomer. The conformations of p66 and p51 subunits are astonishingly different considering that the 2 proteins have the same amino acid sequence with the exception of the RNase H domain of p66. The p66 subunit has a large cleft, containing the primer/

*This paper is dedicated to the memory of Dean L. Richard.

Reprint requests to: Jacob Lebowitz, Department of Microbiology, 520 CHSB, University of Alabama at Birmingham, Birmingham, Alabama 35294.

template binding and the catalytic sites for DNA polymerization, analogous to that of the Klenow fragment of *Escherichia coli* DNA polymerase I (Joyce & Steitz, 1987). The p51 subunit has no such cleft because the 4 polymerase subdomains occupy completely different relative positions. The conformation of p51 completely buries the residues thought to be involved in catalysis. Interactions between the connection subdomains dominate the dimer interface, but lesser contact interactions also occur between the RNase H and the p51 thumb and connection subdomains and between the p51 fingers and the p66 palm and connection subdomains.

The biochemical data concerning dimer interface interactions is quite limited and conflicting. HIV-1 RT can be dissociated with 20% acetonitrile and reassociation can be initiated by reducing the acetonitrile concentration to 5% (Restle et al., 1990, 1992). This approach revealed that both the DNA polymerase and the RNase H activities of RT are exclusively confined to the dimeric form with both heterodimers and p66 homodimers having comparable enzymatic activities (Restle et al., 1990, 1992). However, p51 self-association is very weak, with low DNA polymerization activity (Restle et al., 1990). Furthermore, there was no apparent evidence of heterodimer dissociation at an RT concentration of 680 nM at 0 °C using HPLC gel exclusion methodology to detect monomers and dimers (Restle et al., 1990). An estimated association constant of 10^9 M^{-1} or greater was made based on the above result (Restle et al., 1990). The acetonitrile-induced dissociation can also be detected from the observed difference in fluorescence spectra for the dimer and monomer subunits, and a value of $1.47 \times 10^8 \text{ M}^{-1}$ was obtained at 25 °C in support of the value cited above (Divita et al., 1993b). In contrast to the above result, a K_a value of $4.92 \times 10^5 \text{ M}^{-1}$ at 5 °C was determined using sedimentation equilibrium analysis (Becerra et al., 1991). The latter study also analyzed p66p51 formation at different NaCl concentrations by an immunoprecipitation assay and found that heterodimer formation was apparently not affected by 1.125 M NaCl. Becerra et al. (1991) contend that these results suggest that p66p51 formation has a large hydrophobic component because significant ionic interactions should have been neutralized by greater than 1 M NaCl, thereby resulting in dissociation. No attempt was made to confirm the ionic-strength results by sedimentation equilibrium or velocity measurements (Becerra et al., 1991).

Because dimerization is required to generate a functional enzyme, it has been suggested that agents that can bind at the dimer interface and prevent subunit association could represent a novel therapeutic approach to stem the progression of AIDS (Restle et al., 1990; Babe et al., 1992; Nanni et al., 1993). Very recently, several peptides derived from the connection domain have been shown to inhibit the dimerization of RT (Divita et al., 1994). To extend this approach, it is extremely important to establish the strength and nature of the protein-protein interactions involved in stabilizing the p66p51 heterodimer. The limited number of studies and conflicting data on RT heterodimer stability warranted further studies to examine the association of HIV-1 RT as a function of temperature and ionic strength. We have discovered that heterodimer association is only moderately stable at 5 °C and 20 °C. To our surprise, RT, in 50 and 100 mM Tris, pH 7.0, completely dissociates at 37 °C, and behaves as an ideal monomeric species. Furthermore, increasing salt concentration leads to full dissociation of HIV-RT as monitored by sedimentation velocity analysis. The temperature and ionic strength

dependence of the p66p51 association strongly supports a major role for electrostatic interactions in stabilizing the HIV-1 RT heterodimer.

Results

Sedimentation equilibrium measurements of RT heterodimer stability as a function of temperature at 5, 20, and 37 °C

Sedimentation equilibrium data were obtained for RT at 5 °C and 20 °C in both 50 mM and 100 mM Tris buffer at pH 7.0, using both the Beckman model E (Rayleigh interference optics) and the XLA (absorption optics) analytical ultracentrifuges. Figure 1 presents the concentration of RT as a function of (radial distance)²/2 for the 5 °C data. Comparable sedimentation equilibrium data obtained at 20 °C are not shown. As described in the Materials and methods, the data were fitted globally with the nonlinear least-squares fitting program (NONLIN). An inset in Figure 1 shows the distribution of the deviations of the concentration (residuals) from the fitted curve. Assuming that each monomer does not self-associate, heterodimer formation from p66 and p51 subunits can be considered to be a self-association of "pseudo" monomers with one-half the molecular weight of the heterodimer. This approach is reasonable because Becerra et al. (1991) found that the p51 monomer did not dimerize, and self-association of the p66 monomer had a dimerization constant of about one-tenth that of the heterodimer. It was found from the NONLIN analysis of the data that a monomer-dimer equilibrium best describes the first association step at 5 °C and 20 °C. No other model for the first association step even nearly fit the data. In addition to the monomer-dimer model, further association was detected and described by 2 models that fit the data equally well, i.e., the monomer-dimer-trimer and monomer-dimer-tetramer models. Although it was not possible to determine 1 best association model for RT, it is clear that there is a higher degree of association beyond dimer present, i.e., a small fraction of either trimers or tetramers can form. The respective association constants and the monomer molecular weights of the successful NONLIN fits are presented in Table 1. The monomer molecular weights for each of these successful fits were in agreement with that calculated for the pseudo monomer. Because the results were very similar at both 50 mM and 100 mM Tris, only the latter results are reported in detail in Table 1.

The dimerization constant found at 5 °C is in good agreement with that found by Becerra et al. (1991) and is of such a magnitude that, at 1 mg/mL total protein concentration, there is only about 28% monomer present. There is a decrease in the dimerization constant upon increasing the temperature to 20 °C no matter which model is chosen for the second association step (Table 1). The fraction of monomer present at 1 mg/mL protein concentration increases to between 30% and 40%, depending on the 20 °C dimerization constant.

Figure 2 shows the sedimentation equilibrium data for RT (100 mM Tris, pH 7.0) at 37 °C. The best fit to the sedimentation equilibrium results obtained at 37 °C at both 50 mM (results not shown) and 100 mM Tris indicates that ideal monomeric species are almost exclusively present with a molecular weight average similar to that of the pseudomonomer. The inset to Figure 2 shows small random deviations of the sedimentation equilibrium data from the exponential fit for ideal monomeric behavior.

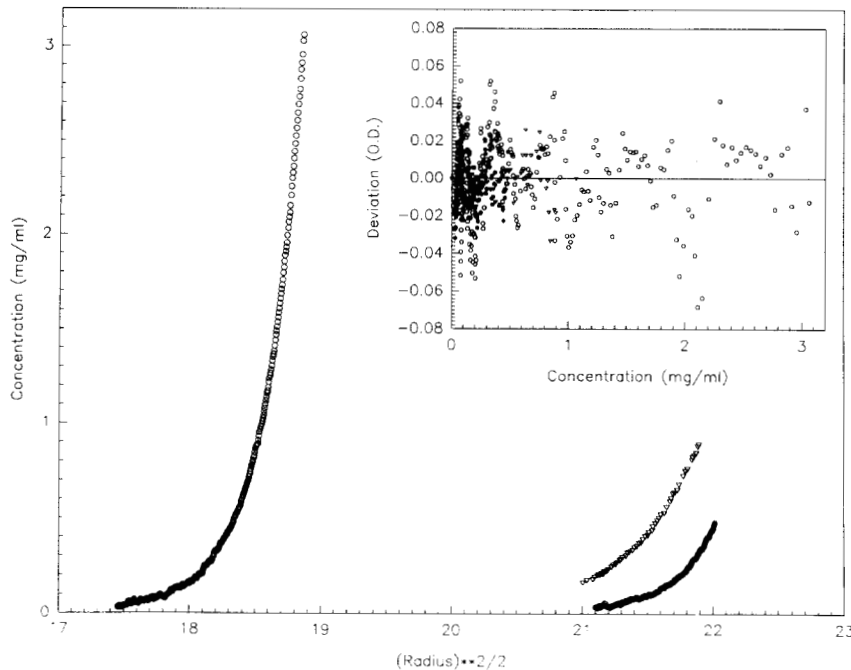


Fig. 1. Rayleigh optics sedimentation equilibrium data at 16,000 rpm obtained for 3 concentrations of HIV-1 RT in 100 mM Tris, pH 7.0, at 5 °C. Concentration distributions of RT as a function of (radial distance)²/2 are: open circles, loading concentration (0.7 mg/mL); open triangles, loading concentration (0.14 mg/mL); and closed circles, loading concentration (0.028 mg/mL). **Inset:** The deviations of the concentration, expressed in OD units, from the exponential fit of the monomer-dimer-trimer model. Symbols correspond to data symbols from the equilibrium concentration distributions given above.

Sedimentation velocity analyses of the dissociation and reassociation of RT as a function of temperature

One can predict the sedimentation velocity coefficients for spherical proteins by combining the Svedberg equation and Stokes equation for the frictional coefficient to obtain Equation 1 (Teller et al., 1979).

$$s = 0.010M^{2/3} \frac{(1 - \bar{v}\rho)}{\bar{v}^{1/3}}, \quad (1)$$

where M equals the molecular weight and \bar{v} and ρ are the partial specific volume of the protein and density of the sedimentation solvent, respectively. Using Equation 1, we predict $s_{w,20}$

values of 7.44S and 4.68S for the heterodimer and monomers (weight average), respectively. Sucrose density gradient analysis of RT was able to partially resolve monomers from the major heterodimer component, and we obtained $s_{w,20}$ values of 7.1S and 4.9S for the heterodimer and monomer peak positions, respectively, relative to a β -amylase 8.9S marker (results not shown). Within experimental error, the measured $s_{w,20}$ values are in good agreement with the hydrodynamic behavior anticipated for essentially spherical heterodimer and monomer molecules. The limited asymmetry shown in the crystal structure for monomers and dimers would not be detected by the $s_{w,20}$ measurements.

Based on the dissociation of RT at 37 °C observed by sedimentation equilibrium, we would anticipate that the stability of

Table 1. Results of best fits for HIV-1 RT at indicated temperatures in 100 mM Tris buffer, pH 7.0^a

Temperature	Association constants			M_1^c (kDa)
	Monomer-dimer	Monomer-trimer ^b	Monomer-tetramer ^b	
5 °C	$5.2 \pm 0.5 \times 10^5$	4×10^9	—	56.4 ± 0.7
	$5.2 \pm 0.5 \times 10^5$	—	1×10^{14}	56.4 ± 0.7
20 °C	$2.1 \pm 1.7 \times 10^5$	4×10^9	—	54.6 ± 0.7
	$3.8 \pm 0.4 \times 10^5$	—	5×10^{13}	56.0 ± 0.7
37 °C	No association detectable— ideal single component	—	—	58.5 ± 4.3

^a For respective monomer to n -mer equilibria, units are $M^{(-n+1)}$. Dimer to trimer K_a values are $7.7 \times 10^3 M^{-1}$ and $1.9 \times 10^4 M^{-1}$ at 5 °C and 20 °C, respectively. Dimer to tetramer K_a values are $3.7 \times 10^2 M^{-1}$ and $3.5 \times 10^2 M^{-1}$ at 5 °C and 20 °C, respectively.

^b Confidence limits extremely large and unsymmetrical.

^c Monomer molecular weight predicted for given association model, to be compared with the calculated monomer molecular weight (from amino acid composition) of the 1/2 heterodimer, i.e., 57.1 kDa.

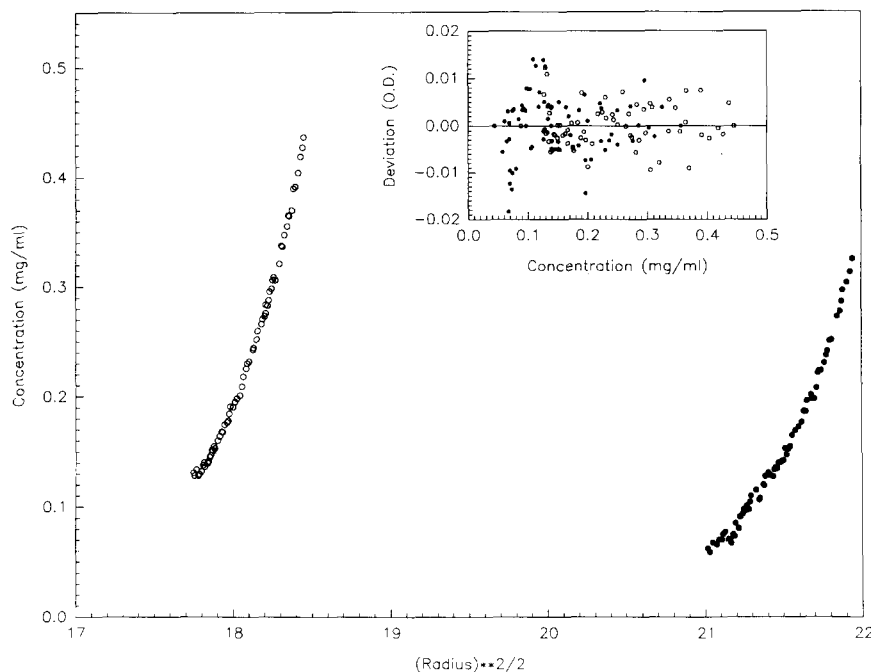


Fig. 2. Absorbance optics sedimentation equilibrium data at 12,000 rpm obtained for 2 concentrations of HIV-1 RT in 100 mM Tris, pH 7.0, at 37 °C. Concentration distributions of RT as a function of (radial distance)²/2 are: open circles, loading concentration (0.7 mg/mL); and closed circles, loading concentration (0.4 mg/mL). **Inset:** The deviations of the concentration, expressed in OD units, from the single-component ideal exponential fit. Symbols correspond to data symbols from the equilibrium concentration distributions given above.

the heterodimer should decrease as a function of increasing temperature from 20 °C to 37 °C with a concomitant decrease in $s_{w,20}$ for RT. This prediction was realized. Band sedimentation velocity analysis (Vinograd et al., 1963) revealed the progressive dissociation of the heterodimer as monitored by a decrease in $s_{w,20}$ from approximately 7.10S to 5.65S from 21 °C to 37 °C (dashed curve, Fig. 3). Based on an anticipated 4.7S weight average $s_{w,20}$ value for monomers, full dissociation of RT did not appear to have been obtained at 37 °C. However, the RT samples were only incubated at each indicated temperature for approximately 70 min, and equilibrium may not have been achieved during this time, compared to 36 h for the sedimentation equilibrium analysis. To test this hypothesis, we incubated RT samples at 20, 27, and 30 °C for 36 h, and sedimentation velocity experiments were performed at each of the indicated temperatures (solid line curve, Fig. 3). It is evident that a 36-h temperature incubation leads to a sharp decrease in sedimentation velocity. An $s_{w,20}$ value of 2.56S was obtained at 30 °C, which is well below the $s_{w,20}$ value for monomers, indicating that complete dissociation and some monomer unfolding had occurred during the long temperature incubation period. No degradation of enzyme was evident from an SDS gel electrophoresis analysis of the 30 °C RT sample (results not shown). From the 37 °C nonequilibrium $s_{w,20}$ value of 5.65S, we estimate that the fraction of dimers present at 70 min was 0.40 using the values of 7.1S and 4.7S for complete association and dissociation, respectively. From first-order dissociation kinetics ($\ln(0.40/4,200)$), we calculate a dissociation rate constant of $2.2 \times 10^{-4} \text{ s}^{-1}$ and a $t_{1/2}$ of 53 min at 37 °C. It would require 5.8 h to achieve 99% dissociation. From the 27 °C nonequilibrium $s_{w,20}$ value of 6.5S, the fraction of dimers present at 70 min was 0.75, and we estimate a dissociation rate constant of $6.85 \times 10^{-5} \text{ M}^{-1} \text{ s}^{-1}$. The fraction of dimers at 27 °C, after 36 h, is estimated to be 0.08 from the $s_{w,20}$ value of 4.92S. From the above 27 °C rate constant, this level of subunit dissociation would require 10.3 h.

The above rough estimates of dissociation rate constants point out that the 36-h incubation period was far in excess of the time needed for full dissociation. The results presented in Figure 3 and the sedimentation equilibrium data provide conclusive evidence for temperature-induced dissociation of HIV-1 RT in 50 and 100 mM Tris buffer at pH 7.0.

Heterodimer reversibility was examined by incubating RT samples at 37 °C for 19 h and 47 h, respectively, followed by a

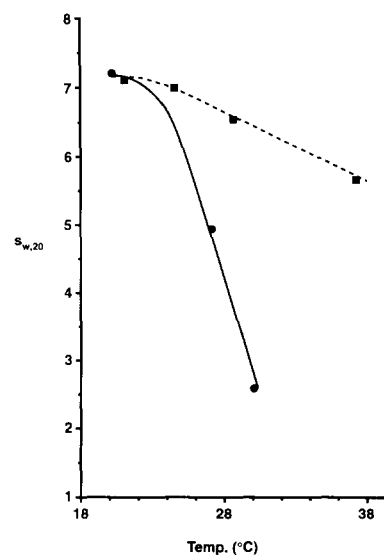


Fig. 3. Sedimentation velocity ($s_{w,20}$) of HIV-1 RT as a function of temperature. Band sedimentation velocity analysis of RT was performed in the model E analytical ultracentrifuge at the indicated temperatures. The dashed and solid curves represent RT temperature incubation at the indicated temperatures for approximately 70 min and 36 h, respectively.

temperature quench to 0 °C for approximately 1 h, and band sedimentation velocity analysis at 20 °C to evaluate the extent of reassociation of monomers. Values of $s_{w,20}$ of 6.45S and 6.77S were obtained for the respective experiments, indicating that substantial reassociation occurred.

Sedimentation velocity analysis of the dissociation of RT as a function of NaCl concentration

To examine the effect of ionic strength on p66p51 association, we determined the changes in $s_{w,20}$ as a function of NaCl concentration (Fig. 4). It is evident that there is a sharp decrease in $s_{w,20}$ between 0.10 and 0.5 M NaCl, leading to apparent complete dissociation based on the $s_{w,20}$ values obtained.

An average $s_{w,20}$ value of 3.6S was obtained for monomer subunits between 0.5 and 1.0 M NaCl (Fig. 4), which is significantly below the anticipated weight average $s_{w,20}$ for spherical monomers of 4.7S. We have observed variability in the stability of different RT preparations and were concerned that proteolytic cleavage sites could be present in the heterodimer, with peptide release occurring upon monomer formation. A reduction of the molecular weight for monomers after salt-induced dissociation could account for the observed lower $s_{w,20}$ values. SDS-gel electrophoresis analysis of the RT samples was used to test this hypothesis (Fig. 5). RT before and after exposure to 1.0 M NaCl showed intact p66 and p51 polypeptides and very low amounts of smaller molecular weight peptides. Consequently, the lower than anticipated $s_{w,20}$ values obtained for monomers is not due to molecular weight changes upon dissociation. The variability of the higher salt $s_{w,20}$ values could be due simply to much larger experimental error in the measurements due to the increased boundary spreading caused by the smaller diffusion coefficient of monomers. It was possible to examine this question, at a later date, with another preparation of RT. RT samples in 0.5–1.0 M NaCl were analyzed in an XL-A analytical ultracentrifuge using a graphical methodology that

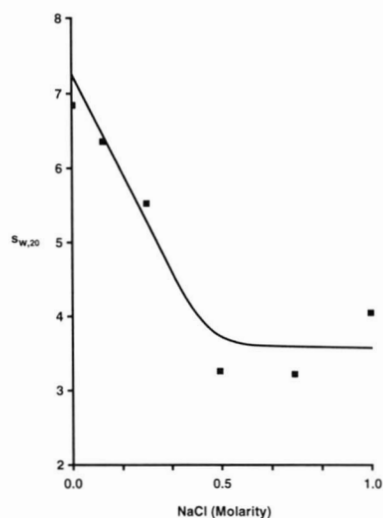


Fig. 4. The sedimentation velocity ($s_{w,20}$) of HIV-1 RT as a function of NaCl concentration. Boundary sedimentation velocity analysis was performed in the model E analytical ultracentrifuge as a function of the indicated NaCl concentrations.

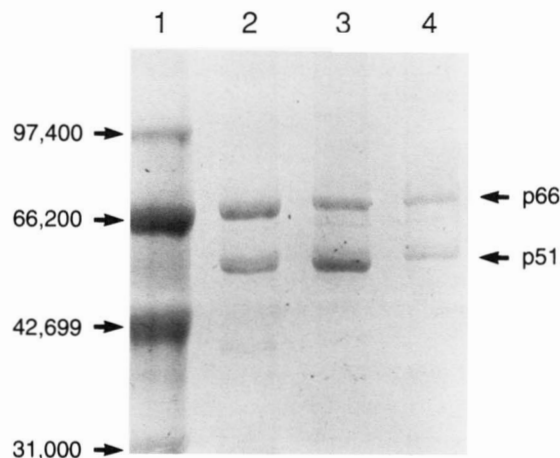


Fig. 5. SDS-PAGE analysis of the molecular weight integrity of RT subunits before and after exposure to 1.0 M NaCl. Lane 1, molecular weight markers by decreasing molecular weight: rabbit muscle phosphorylase *b*, bovine serum albumin, hen egg white, ovalbumin, and bovine carbonic anhydrase. Lane 2, electrophoretic analysis of 30 μ g of RT that was affinity purified using a single-strand DNA column as described in the Materials and methods. Lane 3, electrophoretic analysis of 30 μ g of RT from the 1.0 M NaCl velocity sedimentation analysis dialyzed against 20 mM Tris, pH 7; single-strand DNA affinity purified and dialyzed; and concentrated into 20 mM Tris, 50 mM NaCl, pH 7. RT was stored at -20 °C before analysis. Lane 4, electrophoretic analysis of 6 μ g of RT from the 1.0 M NaCl velocity sedimentation analysis and treated similarly to the RT sample in lane 3 but finally dialyzed against double-distilled H_2O . RT was stored at 4 °C before analysis.

removes boundary spreading due to diffusion (Van Holde & Weischet, 1978). The boundary $s_{w,20}$ values measurements by the Van Holde and Weischet analysis gave consistent values between 4.4S and 4.6S, and the integral distribution of $s_{w,20}$ values showed essentially complete homogeneity at each salt concentration. It appears that the observed variability of the plateau region of Figure 4 is due to the experimental error in the measurement of the midpoints of boundary from recorder traces. We conclude that increasing the ionic strength induces full dissociation of RT without any significant conformational change in the monomers.

Discussion

To extend the analysis of HIV-1 RT heterodimer stability, we first examined the p66p51 subunit association as a function of temperature using sedimentation equilibrium analysis. Association constants were evaluated from the sedimentation equilibrium data using the NONLIN regression analysis. Monomer-dimer-trimer and monomer-dimer-tetramer models fit the data equally well and gave an identical heterodimer K_a value at 5 °C of $5.2 \times 10^5 M^{-1}$ (Table 1). This result is in excellent agreement with the K_a value of $4.9 \times 10^5 M^{-1}$ obtained from sedimentation equilibrium analysis by Lewis using a monomer-dimer model (Becerra et al., 1991). The heterodimer K_a value at 20 °C was $2.1 \times 10^5 M^{-1}$ and $3.8 \times 10^5 M^{-1}$ for the respective association models (Table 1). The sedimentation equilibrium and gel filtration results from Becerra et al. (1991) strongly support only a moderately stable heterodimer at 5 °C and 20 °C. The sedimentation

equilibrium results cannot be easily reconciled with reports of a very stable heterodimer with a K_d value of $1.5 \times 10^8 \text{ M}^{-1}$ at 25°C , which was obtained by dissociating RT with acetonitrile (Restle et al., 1990; Divita et al., 1993b). The latter study used the changes in intrinsic protein fluorescence between dimers and monomers to determine K_d values from the fraction of monomers present at different percentages of acetonitrile. These K_d values were converted into ΔG values and ΔG_d values were extrapolated to zero acetonitrile concentration to obtain the ΔG_d and K_d value in water. This analysis assumes only monomer and dimer states in the presence of different amounts of acetonitrile and is dependent on the validity of the extrapolation to 0% acetonitrile.

Based on sedimentation equilibrium data, the interactions between RT subunits appear completely disrupted at 37°C with the generation of monomers (Fig. 2; Table 1). The dissociation of RT as a function of increasing temperature was also detected by monitoring the decrease in $s_{w,20}$ (Fig. 3). RT also appears to be completely dissociated by increasing the ionic strength of the solution based on the observed decrease in $s_{w,20}$ between 0.10 and 0.5 M NaCl (Fig. 4). Based on the temperature and ionic strength-induced dissociation of RT, electrostatic and hydrogen bond interactions appear to provide very substantial contributions to heterodimer stability.

Becerra et al. (1991) contend that the p66p51 formation has a large hydrophobic component based on the inability to induce dissociation by increasing the NaCl concentration to more than 1.0 M. Becerra et al. (1991) analyzed p66p51 formation at different NaCl concentrations by an immunoprecipitation experimental design involving the detection of ^{35}S -p51 only when complexed with p66. A careful consideration of this experimental design reveals a serious problem: immunoprecipitation of p66/ ^{35}S -p51 over an extended time period of 16 h sets up a coupled reaction that continuously drives the monomer to dimer equilibria toward the formation of heterodimer. This situation would lead to equivalent ^{35}S -p51 immunoprecipitation at different NaCl concentrations even though K_d values were significantly decreased by increasing the ionic strength. Hence, the immunoprecipitation experimental design would not detect the effects of increased ionic strength. Becerra et al. (1991) made no attempt to confirm the immunoprecipitation results by sedimentation equilibrium or velocity measurements.

How can we account for an active enzyme at physiological temperature if free RT appears to completely dissociate into subunits at 37°C ? RT-primer/template association and rate constants have been determined in a number of studies using kinetic methods (Huber et al., 1989; Kati et al., 1992; Reardon, 1992; Beard & Wilson, 1993; Hsieh et al., 1993). For example, Kati et al. (1992) and Hsieh et al. (1993) measured the K_d for primer/template binding at 37°C using the burst amplitude of single nucleotide incorporation and obtained values of 26 nM and 4.7 nM, respectively. A K_d value of <1 nM was obtained by Beard and Wilson (1993). Divita et al. (1993a) obtained a K_d value of 1.8 nM at 25°C from a titration curve that measured binding from the observed changes in intrinsic protein fluorescence. It is evident that a variety of experimental approaches yield K_d values for primer/template binding that are predominantly in the low nanomolar range. Measurement of RT dissociation rates from primer/templates can be made by trapping free RT with an excess competitor. From the dissociation rate constant and K_d values, binding rate constants in the range of

10^6 – $10^7 \text{ M}^{-1} \text{ s}^{-1}$ are obtained (Kati et al., 1992; Beard & Wilson, 1993; Hsieh et al., 1993). Stopped-flow kinetics gives a value of $5 \times 10^8 \text{ M}^{-1} \text{ s}^{-1}$ (Divita et al., 1993a). Given the slow rate of dissociation of free RT heterodimers to monomers, an estimated $t_{1/2}$ of 53 min at 37°C , the primer/template binding step is kinetically isolated. The stability of the binary complex and its rapid rate of formation accounts for enzymatic activity at 37°C . In vivo there are 40–110 RT molecules per virion for other retroviruses (Varmus & Swanstrom, 1984) and one would anticipate similar values for HIV-1. From the volume of the virion, one can calculate a concentration of 14 mg/mL for 50 RT dimers, or $1.23 \times 10^{-4} \text{ M}$. This concentration of RT ensures that the primer site is bound with enzyme.

It should also be emphasized that we have determined heterodimer association constants for RT only in 50 and 100 mM Tris, pH 7.0. Divita et al. (1993b) have found that 10 mM Mg^{2+} enhances the heterodimer association by 100-fold. It is of obvious importance that we extend our sedimentation analysis to examine the effects of Mg^{2+} coupled with other environmental parameters.

Recombinant HIV-1 RT heterodimers for these studies were prepared by mixing *E. coli* cultures separately expressing the p66 and p51 subunits (see Materials and methods). The primary sequence of the recombinant enzyme is identical to the viral RT. Bacterially expressed HIV-1 p66 homodimers are very sensitive to proteolytic cleavage, leading to the formation of p66p51 heterodimers (Larder et al., 1987; Lowe et al., 1988; Clark et al., 1990; Thimmig & McHenry, 1993). Although both protease processing of p66 homodimers and p66+p51 subunit association yield active enzyme, structural variations in heterodimers could be envisioned based on possible subunit isomerization differences in forming heterodimers by different mechanisms. A comparative examination of the stability of heterodimers generated by proteolytic processing versus heterodimers formed from separate subunits would resolve whether there are differences in dimer interface interactions based on differences in heterodimer assembly pathways. The identification of the major stabilizing interactions at the dimer interface would open the possibility of developing potential dissociative inhibitors of RT.

Materials and methods

Materials

Deuterium oxide (99.5%) was obtained from Aldrich. [Methyl- ^3H]thymidine 5'-triphosphate (specific activity 41 Ci/mmol) was obtained from Amersham. All other chemicals used in the study were reagent grade.

Methods

HIV-1 RT preparation, DNA polymerization assay, and reconstitution of active enzyme from high salt

The laboratory of Dr. Casey D. Morrow and the Center for AIDS Research Protein Expression Core Facility of UAB created plasmids for separate expression of HIV-1 RT (viral strain BH10) p66 and p51 subunits utilizing the T7 RNA polymerase promoter of the plasmid. HIV-1 RT heterodimer was prepared as follows. Separate cultures of *E. coli* strain BL21(DE3), which has the T7 RNA polymerase gene inserted on the chromosome,

under control of the *lac* promoter, were transformed with the p51 and p66 pET plasmids and selected for phenotypic expression of antibiotic resistance genes. Following transformation, the cells were grown to midlog phase and the T7 RNA polymerase was induced by the addition of isopropyl β -D-thiogalactopyranoside. After 3 additional hours of growth at 37 °C, the *E. coli* cells were collected by centrifugation and sonicated together. The resulting supernatant was loaded onto a phosphocellulose column at 4 °C. The column was washed overnight with 75 mM KCl, 50 mM Tris, pH 7.0, 1 mM EDTA, 10% glycerol, and 5 mM β -mercaptoethanol. The RT was then eluted with 150 mM KCl, precipitated with ammonium sulfate, and concentrated. The enzyme was stored in 50 mM Tris, pH 7.0, at 4 °C. Protein concentrations were determined by measuring the absorbance at 280 nm in a Cary 210 spectrophotometer using a heterodimer value of 1.17 A_{280} for 1 mg/mL, which is based on the weight fractions of the extinction coefficients of 1.36 and 0.93 A_{280} for 1-mg/mL solutions of purified p66 and p51, respectively (Becerra et al., 1991).

The sedimentation equilibrium experiments were performed with 2 different preparations of the enzyme. The $s_{w,20}$ versus temperature, nonequilibrium, and equilibrium experiments were performed with 3 different preparations of RT and the $s_{w,20}$ versus NaCl was performed with a separate preparation of RT.

The DNA polymerase activity of RT was determined by measuring time-dependent incorporation of thymidine into a poly-dT primer as follows. Poly(A)_{1,000}·(dT)₁₅ (Boehringer Mannheim GmbH) was used as the primer template for RT and was diluted in 50 mM Tris·HCl, 5 mM Mg²⁺, pH 7.0, to a concentration of 1.8 μ g/mL. One microliter of RT stock solution (2–10 mg/mL) was preincubated with the primer template for 10 min before starting the polymerization reaction by adding 1,098 pmol of [³H]TTP, having a specific activity of 41 Ci/mmol, in a total reaction volume of 600 μ L. Reactions were carried out at room temperature (approximately 23 °C) and 37 °C. The amount of incorporation of tritium was measured by taking aliquots at 30-s intervals and stopping the reaction in the presence of 167 mM EDTA. The quenched reaction mixture was spotted on DE81 filter paper, washed with 0.3 M ammonium formate and 95% ethanol, and counted in a liquid scintillation counter. As a control, aliquots of the reaction mixture without the enzyme were quenched with EDTA, spotted on DE81 paper, washed, and counted. The conversion of cpm data into picomoles incorporated was determined from a calibration plot of cpm versus picomoles for known quantities of [³H]TTP added to the DE81 filter paper. Using freshly prepared RT and newly purchased [³H]thymidine triphosphate and poly-(rA):dT₁₅, we obtained the following k_{cat} values: 0.39, 0.38, 0.40, and 0.43, with R^2 values greater than 0.99. The first 3 experiments were at room temperature and the fourth at 37 °C. Additional cold TTP was added in experiments 3 and 4 without affecting the rate, indicating that [³H]dTTP was saturating.

RT that was dissociated by 1.0 M NaCl was reconstituted into heterodimers by a combination of dialysis and DNA affinity purification. DNA affinity columns were prepared by incubating biotinylated single-stranded DNA with beaded agarose cross-linked with streptavidin (Pierce). The streptavidin agarose slurry was packed in 1-mL syringes that were plugged with glass wool and washed several times with 0.02% sodium azide solution. The columns were then saturated with biotinylated single-stranded DNA and stored in 0.02% sodium azide at 4 °C. Prior to bind-

ing RT, the columns were washed several times with the same buffer the protein was to be dialyzed into, 20 mM Tris, 50 mM NaCl, pH 7. RT in 1.0 M NaCl was dialyzed against the latter buffer. The protein was then loaded onto the DNA affinity column, followed by a couple of washes with the dialysis buffer. Absorbance measurements of the washes indicated that RT was completely bound by the single-stranded DNA. RT was then eluted with 20 mM Tris, 200 mM NaCl, concentrated, and dialyzed against 20 mM Tris, 50 mM NaCl, pH 7, for storage. The molecular weight integrity of RT subunits before and after exposure to 1.0 M NaCl was examined using SDS-PAGE analysis (Laemmli, 1970).

Analytical ultracentrifuge analyses

Sedimentation equilibrium analysis of RT. Sedimentation equilibrium experiments were performed at the National Analytical Ultracentrifuge Facility at the University of Connecticut. A Beckman Model E Analytical Ultracentrifuge equipped with on-line data acquisition (Yphantis, 1979; Laue, 1992) was used for the 5 °C and 20 °C sedimentation experiments. Two 2-mm double-sector cells were loaded with solutions of RT (in 50 mM and 100 mM Tris, pH 7.0) at a concentration of 2.1 mg/mL. In addition, two 6-channel cells were loaded with 0.7, 0.14, and 0.028 mg/mL of RT at the 2 buffer concentrations cited above. Centrifugation was performed at 16,000 rpm. Data were taken in terms of fringe displacement as a function of radial distance every 0.01 mm. A Beckman XL-A analytical ultracentrifuge utilizing absorption optics was used for sequential temperature studies of RT at 5, 20, and 37 °C. Two 6-channel cells were loaded with 0.7, 0.4, and 0.2 mg/mL of RT at the 2 ionic strengths to a column height of ca. 2.5 mm and then centrifuged to equilibrium at 12,000 rpm. The data were taken in absorbance units (AU) at 280 nm as a function of radial distance every 0.01 mm. Equilibrium was considered to have been achieved when 2 sets of data taken every 4 h agreed with an RMS difference within 0.02 fringes or 0.01 AU with no observable systematic deviation. Equilibrium was achieved with a column height of solvent ca. 2.5 mm within 36 h.

For a self-associating system, monomer to n -mer at sedimentation equilibrium, the total solute concentration at any radial position (r) in the centrifuge cell is the sum of the monomer to n -mer species. This sum can be expressed as the free monomer concentration $C_1 = (C_1)_0 \exp[M_1(1 - \bar{v}\rho)(\omega)^2(r^2 - r_0^2)/2RT]$ plus the concentration of each n -mer species, where $(C_n) = K_n(C_1)_0^n \exp[nM_1(1 - \bar{v}\rho)(\omega)^2(r^2 - r_0^2)/2RT]$. $(C_1)_0$ equals the monomer concentration at r_0 , the reference radius; K_n is the association constant for the formation of n -mer from monomer; M_1 is the monomer molecular weight; \bar{v} and ρ are the partial specific volume of the protein and density of the sedimentation solvent, respectively; ω is the angular velocity; R is the gas constant; and T is the temperature in Kelvin. Exponential terms for dimer, trimer, tetramer, etc. can be included and modified to include the effects of nonideality. If $(C_1)_0$ and $K_n(C_1)_0^n$ are expressed as $\exp[\ln(C_1)_0]$ and $\exp[\ln K_n(C_1)_0^n]$, then the concentration value and association constants are constrained to positive values. A nonlinear regression analysis of the total concentration as a function of radial distance r^2 or $r^2/2$ can be performed to determine the monomer molecular weight, association constants, stoichiometries, and nonideality coefficients for selected association models that best fit the data. For a detailed introduction and discussion of the modeling of self-associating

systems in the analytical ultracentrifuge, the reader should consult McRorie and Voelker (1993).

Data analysis was performed using the nonlinear least-squares program, NONLIN (Johnson et al., 1981). The combination of several sets of data over a wide range of experimental conditions is preferred in order to obtain a unique solution or fit to the data. In this case, the data from both optical systems (fringes and absorbance values are converted to a concentration scale) were combined when available. This resulted in ca. 560–610 data points at 5 °C and 20 °C, and about 135 data points for the 37 °C study. The range of concentration distribution was from as low as a few micrograms/milliliter to as high as 3 mg/mL for these solutions. This concentration range results from the depleting effect at the meniscus and the concentrating effect at the bottom of the cell due to the centrifugation process.

In order to perform a global fit by combining all the data taken at different speeds and loading concentrations, one must use speed factors that are proportional to the square of the running speeds and concentration factors that are equal to the concentration in milligrams/milliliter, which can produce an optical density or a fringe displacement of 1 for the particular cell and wavelength. A simple model (i.e., a single ideal species) was first fitted to the combined sets of data from the different sample loading concentrations and speeds of rotation. This analysis yields a value of $M' = M(1 - \bar{v}\rho)$, which for this model is the Z average molecular weight (D. Yphantis, pers. comm.). The criteria for goodness of fit are that the RMS error be small (usually about 0.02 of a fringe or 0.01 of an AU, which is, assuming a typical refractive increment or extinction coefficient, equivalent to about 7–20 $\mu\text{g/mL}$) and that it be random, i.e., have a small systematic error in the residuals.

The second model tried was that of a single nonideal species. This yields the value of M' and the degree of nonideality (the second virial coefficient B), which in turn gives information regarding possible association or effective charge. The third model tried, that of the monomer–dimer, which yields the value of M' for the associating monomer (M_1) and the natural logarithm of the association constant. Further fits tried were monomer–trimer, monomer–dimer–trimer, monomer–tetramer, monomer–dimer–tetramer, etc.

In order to convert values of M' into molecular weight, one needs to know the partial specific volume of the molecule in its solvent and the density of the solvent. It is possible to estimate the value of \bar{v} fairly accurately from amino acid composition data (Cohn & Edsall, 1943). This was found to be 0.717 mL/g for the heterodimer. The densities of solvents were estimated from density tables to be 1.003, 1.001, and 0.998 g/mL at 5, 20, and 37 °C, respectively, for 100 mM Tris buffer and 1.002, 1.000, and 0.997 at the same temperatures for 50 mM Tris buffer.

Sedimentation velocity analysis of RT. Sedimentation velocity measurements were performed on a Beckman model E analytical ultracentrifuge equipped with photoelectric scanners. An extra heater wire was added to the model E rotor temperature control unit in order to readily obtain temperatures above 32 °C for the sedimentation analysis described below. Boundary and band sedimentation was performed in an aluminum rotor (type AnD) at 56,000 rpm at indicated temperatures using a double-sector centerpiece. Recorder tracings of the absorbance of the moving boundary or band were made at regular time intervals

on the instrument's Dynograph recorder. A wavelength between 280 nm to 295 nm was selected depending on the concentration of RT in the cell. For boundary sedimentation velocity analysis, the movement of the midpoint (r) of the absorbance boundary vs. time (t) was used to obtain the uncorrected sedimentation coefficient s^* from the slope of the plot of $\ln r$ versus t divided by ω^2 , i.e., $(d \ln r)/\omega^2 dt$. The standard correction equation (Equation 2) was used to convert s^* values to $s_{w,20}$ values:

$$s_{w,20} = s^* \frac{(\eta)_{T,b}}{(\eta)_{w,20}} \cdot \frac{(1 - \bar{v}\rho)_{w,20}}{(1 - \bar{v}\rho)_{T,b}}, \quad (2)$$

where η is the viscosity for water at 20 °C (designated by subscripts $w,20$) or the viscosity for the buffer at the temperature of the sedimentation velocity experiment (designated by subscripts T,b). The values of the partial specific volume of the protein and solvent density in water at 20 °C or under the buffer and temperature conditions of the experiment are used in the buoyancy term $(1 - \bar{v}\rho)$ as designated by the subscripts. However, because experimental values of \bar{v} are not readily obtained, we exclusively used the amino acid compositional value for RT of 0.717 in Equation 2. The density and viscosity corrections for different concentrations of NaCl were made using the polynomial equations and tables of coefficients for these polynomials in Laue et al. (1992).

Band sedimentation (Vinograd et al., 1963) of RT was used to evaluate the changes of $s_{w,20}$ as a function of temperature. A double-sector band-forming centerpiece was used for this analysis. In this cell, 15–20 μL of RT (3–6 mg/mL) was transferred, through a channel, from a small well to the sample sector solution (D_2O containing 50 mM Tris, pH 7.0) upon the initiation of centrifugation. A self-generating density gradient caused by diffusion of D_2O into the thin lamella of protein solution prevents convection thereby stabilizing the macromolecules in a sedimenting band or zone. A wavelength between 290 nm and 300 nm was selected depending on the concentration of RT in the cell. Tracings of zone movement were recorded as a function of time, and the radial position of the symmetric midpoint of the Gaussian profile of the zone was measured at each time interval. The uncorrected sedimentation coefficient was determined as described above for boundary sedimentation. The initial study of the sedimentation velocity of RT as a function of temperature was performed as follows: (1) the band well was filled with 20 μL of RT in 50 mM Tris, pH 7.0, and the cell assembled; (2) the density gradient solvent, D_2O (50 mM Tris, pH 7.0), was then loaded in both sectors of the centerpiece; (3) the centrifuge cell and rotor were incubated in a constant temperature incubator and upon reaching a temperature close to the value desired, the rotor was then loaded into the Model E; and (4) centrifugation was initiated upon reequilibration to the desired temperature. This experimental set-up required approximately 70 min. Equation 2 was used to obtain $s_{w,20}$ values from the observed s values. The density and viscosity of D_2O at each temperature was determined using the polynomial equations and tables of coefficients for these polynomials in Laue et al. (1992). Upon discovery that a 70-min incubation time did not appear to have attained chemical equilibrium, we incubated RT samples at 20, 27, and 30 °C for 36 h to test this hypothesis.

The original application of band centrifugation showed good agreement between band and boundary analysis using Equation 2

(Vinograd et al., 1963). Good agreement was also obtained for RT between band and boundary analysis using Equation 2. However, it should be pointed out that Belli (1973) found for the band centrifugation of ribosomes in D₂O that Equation 2 overestimated $s_{w,20}$ by 17%. A comparable overestimate of $s_{w,20}$ was obtained by us for β -amylase in D₂O relative to the boundary $s_{w,20}$ value (Englard & Singer, 1950). Consequently, we raise a cautionary note regarding the use of Equation 2 for obtaining $s_{w,20}$ values from band centrifugation in D₂O without a boundary comparison in an H₂O buffer.

Acknowledgments

These studies were supported by the UAB AIDS Center NIH grant P30 AI 27767 and travel funds from the UAB Department of Microbiology to perform the sedimentation equilibrium analysis at the National Analytical Ultracentrifuge Facility at the University of Connecticut. This facility is supported by NSF grant DIR-8717034. We gratefully thank Chao-ying Zhang for technical and data processing assistance. S.K. was supported by a stipend from the Biophysical Science Program under the direction of Dr. Herb Cheung. D.L.R. was partially supported by a Cystic Fibrosis Foundation Pilot Grant. We thank Dr. Eric Sorscher for additional support of D.L.R. We gratefully thank Drs. Jeff Hansen and Borries Demler for providing a Van Holde-Weischet analysis of RT at high salt concentrations. We also thank Mamoun Eltahir for the SDS-PAGE analysis of RT.

References

- Babe LM, Rose J, Craik CS. 1992. Synthetic "interface" peptides alter dimeric assembly of the HIV 1 and 2 proteases. *Protein Sci* 1:1244-1253.
- Beard WA, Wilson SH. 1993. Kinetic analysis of template-primer interactions with recombinant forms of HIV-1 reverse transcriptase. *Biochemistry* 32:9745-9753.
- Becerra SP, Kumar A, Lewis MS, Widen SG, Abbots J, Karawya EM, Hughes SH, Shiloach J, Wilson SH. 1991. Protein-protein interactions of HIV reverse transcriptase: Implication of central and C-terminal regions in subunit binding. (Lewis MS. Appendix: Ultracentrifuge analysis of a mixed association.) *Biochemistry* 30:11707-11719.
- Belli M. 1973. The evaluation of standard sedimentation coefficient in band sedimentation of macromolecules. *Biopolymers* 12:1853-1864.
- Clark PK, Ferris AL, Miller DA, Hizi A, Kim KW, Deringer-Boyer SM, Mellini ML, Clark AD Jr, Arnold GF, Lebherz WB III, Arnold E, Muschik GM, Hughes SH. 1990. HIV-1 reverse transcriptase purified from a recombinant strain of *Escherichia coli*. *AIDS Res Hum Retroviruses* 6:753-764.
- Cohn EJ, Edsall JT. 1943. *Proteins, amino acids and peptides as ions and dipolar ions*. New York: Reinhold. pp 370-381.
- DiMarzo-Veronese F, Copeland TD, DeVico AL, Rahman R, Oroszlan S, Gallo RC, Sarngadharan MG. 1986. Characterization of the highly immunogenic p66/51 as the reverse transcriptase of HTLV-III/LAV. *Science* 231:1289-1291.
- Divita G, Muller B, Immendorfer U, Gautel M, Rittinger K, Restle T, Goody RS. 1993a. Kinetics of interaction of HIV-1 reverse transcriptase with primer/template. *Biochemistry* 32:7966-7971.
- Divita G, Restle T, Goody RS. 1993b. Characterization of the dimerization process of HIV-1 reverse transcriptase heterodimer using intrinsic protein fluorescence. *FEBS Lett* 324:153-158.
- Divita G, Restle T, Goody RS, Chermann JC, Baillon JG. 1994. Inhibition of human immunodeficiency virus type 1 reverse transcriptase dimerization using synthetic peptides derived from the connection domain. *J Biol Chem* 269:13080-13083.
- Englard S, Singer TP. 1950. Physicochemical studies on β -amylase. *J Biol Chem* 187:213-219.
- Hansen J, Schulze T, Mellert W, Moelling K. 1988. Identification and characterization of HIV-specific RNase H by monoclonal antibody. *EMBO J* 7:239-243.
- Hsieh JC, Zinnen S, Modrich P. 1993. Kinetic mechanism of the DNA-dependent DNA polymerase activity of human immunodeficiency virus reverse transcriptase. *J Biol Chem* 268:24607-24613.
- Huber HE, McCoy JM, Seehra J, Richardson CC. 1989. Human immunodeficiency virus 1 reverse transcriptase. Template binding, processivity, strand displacement synthesis, and template switching. *J Biol Chem* 264:4669-4678.
- Jacobo-Molina A, Ding J, Nanni G, Clark AD Jr, Lu X, Tantillo C, Williams RL, Kamer G, Ferris AL, Clark P, Hizi A, Hughes SH, Arnold E. 1993. Crystal structure of human immunodeficiency virus type 1 reverse transcriptase complexed with double-stranded DNA at 3.0 Å resolution shows bent DNA. *Proc Natl Acad Sci USA* 90:6320-6324.
- Johnson ML, Correia JJ, Yphantis DA, Halvorson HR. 1981. Analysis of data from the analytical ultracentrifuge by nonlinear least squares techniques. *Biophys J* 36:575-588.
- Joyce CM, Steitz TA. 1987. DNA polymerase I: From crystal structure to function via genetics. *Trends Biochem Sci* 12:288-292.
- Kati WM, Johnson KA, Jerva LF, Anderson KS. 1992. Mechanism and fidelity of HIV reverse transcriptase. *J Biol Chem* 267:25988-25997.
- Kohlstaedt LA, Wang J, Friedman JM, Rice PA, Steitz TA. 1992. Crystal structure at 3.5 Å resolution of HIV-1 reverse transcriptase complexed with an inhibitor. *Science* 256:1783-1790.
- Laemmli UK. 1970. Cleavage of structural proteins during the assembly of head of bacteriophage T4. *Nature* 227:680-685.
- Larder B, Purifoy D, Powell K, Darby G. 1987. AIDS virus reverse transcriptase defined by high level expression in *Escherichia coli*. *EMBO J* 6:3133-3137.
- Laue TM. 1992. On-line data acquisition and analysis from the Rayleigh interferometer. In: Harding SE, Rowe AJ, Horton JC, eds. *Analytical ultracentrifugation in biochemistry and polymer science*. Cambridge, UK: Royal Society of Chemistry. pp 63-89.
- Laue TM, Shah BD, Ridgeway TM, Pelletier SL. 1992. Computer aided interpretation of analytical sedimentation data for proteins. In: Harding SE, Rowe AJ, Horton JC, eds. *Analytical ultracentrifugation in biochemistry and polymer science*. Cambridge, UK: Royal Society of Chemistry. pp 90-125.
- Lightfoote MM, Coligan JE, Folks TM, Fauci AS, Martin MA, Venkatesan S. 1986. Structural characterization of reverse transcriptase and endonuclease polypeptides of the acquired immunodeficiency syndrome retrovirus. *J Virol* 60:771-775.
- Lowe DM, Aitken A, Bradley C, Darby G, Larder BA, Powell TL, Purifoy DJM, Tisdale M, Stammers DK. 1988. HIV-1 reverse transcriptase: Crystallization and analysis of domain structure by limited proteolysis. *Biochemistry* 27:8884-8889.
- McRorie DK, Voelker PJ. 1993. *Self-associating systems in the analytical ultracentrifuge*. Fullerton, California: Beckman Instruments.
- Nanni GR, Ding J, Jacobo-Molina A, Hughes SH, Arnold E. 1993. Review of HIV-1 reverse transcriptase three-dimensional structure: Implications for drug design. *Perspect Drug Discovery Design* 1:129-150.
- Reardon JE. 1992. Human immunodeficiency virus reverse transcriptase: Steady state and pre-steady state kinetics of nucleotide incorporation. *Biochemistry* 31:4473-4479.
- Restle T, Muller B, Goody RS. 1990. Dimerization of human immunodeficiency virus type 1 reverse transcriptase. *J Biol Chem* 265:8986-8988.
- Restle T, Muller B, Goody RS. 1992. RNase H activity of HIV reverse transcriptases is confined exclusively to the dimeric forms. *FEBS Lett* 300:97-100.
- Teller DC, Swanson E, DeHaen C. 1979. The translation friction coefficient of proteins. *Methods Enzymol* 61:103-124.
- Thimmig RL, McHenry CS. 1993. Human immunodeficiency virus reverse transcriptase. Expression in *Escherichia coli*, purification, and characterization of functionally and structurally asymmetric dimeric polymerase. *J Biol Chem* 268:16528-16536.
- Van Holde KE, Weischet WO. 1978. Boundary analysis of sedimentation-velocity experiments with monodisperse and paucidisperse solutes. *Biopolymers* 17:1387-1403.
- Varmus H, Swanstrom R. 1984. Replication of retroviruses. In: Weiss R, Teich N, Varmus H, Coffin J, eds. *RNA tumor viruses, 2nd ed*. Cold Spring Harbor, New York: Cold Spring Harbor Laboratory Press. pp 369-512.
- Vinograd J, Bruner R, Kent R, Weigle J. 1963. Band centrifugation of macromolecules and viruses in self-generating density gradients. *Proc Natl Acad Sci USA* 49:902-910.
- Whitcomb JM, Hughes SH. 1992. Retroviral reverse transcription and integration: Progress and problems. *Annu Rev Cell Biol* 8:275-306.
- Yphantis DA. 1979. Pulsed laser interferometry in the ultracentrifuge. *Methods Enzymol* 61:3-12.